ATA Memo #37 — 7 December 2001

Simulations of Narrow-Band Phased-Array Null Formation for the ATA

Geoffrey C. Bower

ABSTRACT

We describe the minimum variance technique for the deterministic calculation of complex gains that will place narrow-band nulls in the response of a beam former while maximizing the signal-to-noise ratio in the source direction. We consider the application of this technique for the ATA. Nulls are $\sim$ 100 kHz in frequency and $\sim 10''$ in angular size at 1.4 GHz. The null angular size decreases with increasing frequency. Multiple nulls can be easily placed to increase the size of the null in a particular region or to null widely separated interferers. The nulls can withstand $\sim 10^\circ$ of phase noise and $\sim 5\%$ of amplitude gain noise. Gains must be updated on timescales less than 100 milliseconds to maintain nulls. We discuss the relative merits of measuring or simulating the correlation matrix which is the basis of the calculation.

1. Narrow-Band Null Formation

Adjusting the complex gains in beam formers can produce multiple nulls on the sky while maintaining gain in the direction of the source. This technique is inherently narrow band. However, the compact configuration of the Allen Telescope Array sets the difference between narrow-band and broadband at a large enough bandwidth to be of interest for a variety of interferers. Many terrestrial communication systems have bandwidths on the order of 10 kHz. Much of the theory for these techniques has been developed for radar and wireless communication problems (e.g., Godara 1997) but it remains applicable to radio astronomy.

The case that we consider begins with an array of N_a antennas at positions $\mathbf{b}_k$. Each antenna receives a signal V_k:

$$V_k = exp(2\pi i f(t - \tau_k^g)), \tag{1}$$

where $\tau_k^g = \mathbf{b}_k \cdot \mathbf{n}$ is the geometric delay corresponding to the source direction $\mathbf{n}$. Mixing this signal with an LO at a frequency f_0 and applying delay correction τ_k^i produces an IF signal V_k':

$$V_k' = exp(2\pi i(f - f_0)t - f\tau_k^g - f\tau_k^i)). \tag{2}$$

The beam former creates a phased output Y that is the complex weighted sum of all V_k':

$$Y = \sum_k g_k exp(2\pi i(f - f_0)t - f\tau_k^g - f\tau_k^i)), \tag{3}$$

where $g_k = w_k exp(i\phi_k)$.

The modulus of Y is the beam power pattern R, which can be shown to be:

$$R = \sum_j \sum_k w_j w_k cos(2\pi f(\tau_j^g - \tau_k^g + \tau_j^i - \tau_k^i) + \phi_j - \phi_k). \quad (4)$$

We set $\tau_k^i = -\tau_k^g(\mathbf{n})$ so that R is only a function of ϕ_k in the direction of the source. This formulation does not take into account the effects of the primary beam. These could be included with a gain term that is a function of $\mathbf{n}$.

The nulling problem is to a place a maximum in the direction n_0 and nulls in the directions $n_l, l = 1, 2, ..., N_i$. This can be written in a matrix formulation:

$$\mathbf{g}^H \mathbf{A} = \mathbf{e}^T, \quad (5)$$

where $\mathbf{A}$ is an array of steering vectors $\mathbf{s}_l = exp(i2\pi f \tau^g)$ and $\mathbf{e}$ is a vector $[1, 0, 0, ..., 0]$ with $N_i + 1$ elements. That is, the response of array is expected to be 1 at n_0 and 0 at $n_l, l > 0$. This equation has solutions for $N_i <= N_a - 1$. However, these solutions do not maximize the SNR in the direction of the source.

With the constraint that the SNR must be maximized, the nulling solution becomes

$$\mathbf{g} = \frac{\mathbf{X}^{-1}\mathbf{n}_0}{\mathbf{n}_0 \mathbf{X}^{-1}\mathbf{n}_0}. \quad (6)$$

$\mathbf{X}$ is the correlation matrix for the array. It can either be estimated using the known positions of the interferers or it can be measured with a correlator. Measuring the correlation matrix introduces noise that can lead to substantial errors in $\mathbf{g}$ for weak interferers (Ellingson & Hampson). Adding the constraint, reduces the number of interferers that can be eliminated to $N_a - 2$. This algorithm is known as minimum variance (MV). It is also referred to as Capon's Beamformer, Constrained Power Minimization and NAME.

2. Simulations of MV

We describe here simulations of MV using a proposed 350-element ATA configuration. The configuration is Bock's k12_1 (Figure 1). The minimum, median and maximum antenna separations are 11, 254 and 878 m.

Since we are adjusting phase not delay, nulls are inherently narrow band under this scheme. An order of magnitude estimate of the bandwidth can be estimated $\Delta\nu = \tau_{max}^{-1}$. In the case of the ATA configuration, $\Delta\nu \approx 350$ kHz. We can measure the actual response by placing a null at a given frequency and then measuring the response of the array at adjacent frequencies in the direction of the interferer. We demonstrate in Figure 2 that the null can be very deep (in this case -130 dB) but that its width is very narrow at these levels[1]. For the example shown, the width is 100 and 200 kHz at levels of -40 and -30 dB, respectively. These numbers are representative. Different nulls can be slightly broader or narrower at these levels, depending on their location on the sky. The frequency width is independent of the observing frequency. Broad band nulling can be accomplished with a filter bank approach.

The angular width of the null scales linearly with wavelength. At 1.4 GHz, the -40 and -50 dB angular widths are on the order of $10''$ and $2''$. For the specific null shown (Figures 3, 4 and 5), the -30 dB width is on the order of $100''$. But as with the frequency width, this width is sensitive to the region on the sky surrounding the null. Note that there are several other nulls in the vicinity of the main null that were not placed by the algorithm.

The width of a null on the sky can be increased by placing multiple nulls in the same region. Placing five nulls in a cross with arm lengths of $16''$ increases the -40 and -50 dB angular widths to $80''$ and $60''$, respectively (Figure 6). The width can be increased with the placement of further nulls.

The effect of the nulling on the main beam shape increases with a number of nulls. For a single null, the maximum deviation from the optimal beam (after scaling of the peak) in the central 4 arcmin is $\sim 0.2\%$ of the beam peak (Figure 8). For 15 nulls, the maximum deviation in the same region is $\sim 1\%$ (Figure 9). Even for 300 nulls, the maximum deviation is a 15% sidelobe. In all cases, the deviation at the beam center is exactly zero. Multiple nulls can be placed across the field with small effect on the beam pattern in other parts of the sky (Figure 7). Complex null patterns can be detailed on the sky (Figure 10).

Nulls can also be interpolated between two or more fixed solutions. However, these solutions are not always accurate, even with second-order interpolation between three solutions (Figure 11). Proper interpolation should probably be done in the correlation matrix domain.

Perturbations of the solutions indicate the robustness against gain instability. An error of $\sim 10°$ leaves the -40 dB contour essentially unchanged. Increasing the error to $\sim 30°$ leads to a substantial probability that the null will be destroyed. Thus, the nulls are essentially as stable as the beam peak. Gradients of phase across the array should correspond to a change in the position of the interferer. Errors in amplitude gain of about 5% preserve -40 dB contours. Replacing the gains with unity destroys the null, even though the gains typically deviate by less than 5%. Perhaps, the significant difficulty that will be encountered with amplitude gains is the variation in gain from antenna to antenna at angles far from the primary beam.

Update times for the complex gains are set by the changing directions of the source and the interferers. As an example, we use the actual position of a GPS satellite as a function of time

[1] Note that our beamformer is normalized to unity in the source direction. Off-source, the mean response is $\sim 1/N$, which is -25 dB for $N = 350$

and show the change in phase and amplitude solutions necessary (Figure 12). In this example, the source direction remains fixed. But to first order, this configuration is similar to the conditions for a changing source position but fixed transmitter. The phase and amplitude solutions change on the same timescale. The structure function plots indicates that the timescale for variation of the complex gain saturates at approximately 100 milliseconds with a maximum of 0.003 in squared amplitude and 9 $\deg^2$ in phase. The update rates are the same whether are for amplitude and phase or real and imaginary gains.

The angular width of the nulls and the ability to precisely place multiple nulls substantially reduce the frequency with which gain solutions must be updated. For a celestial source and a fixed terrestrial interferer, the interferer will stay within the -40 dB boundary for a few seconds. Update times are governed by the frequency with which the main beam is updated. In one example, we placed 50 nulls along the path of a GPS source over $\sim 0.2°$ corresponding to a time interval of 1.5 seconds (Figure 13). The gain phases and amplitudes varied roughly linearly with the sidereal motion of the source. The null depth at the location of the interferer was always lower than -90 dB. In actual use, one could trade-off between number of nulls, mean suppression and update time.

The behvior of the SNR in the source direction for increasing number of nulls is a stron argument for a large-N array. Figure 14 shows that for a 350-element array placing 128 nulls only decreases the SNR to 80% of its maximum. The SNR goes as $1 - \frac{N_{null}}{(2N_{ant}-N_{null}-2)}$. Thus, the ATA can place hundreds of nulls while the VLA could place less than 50.

3. Conclusions

The depth of nulls will be governed by the accuracy with which the array can be phased. Uncorrected ionospheric and trophospheric phase errors place limits on the depth. Updates of these terms on timescales of minutes should be sufficient. Amplitude gain errors may be more important because they are more difficult to control. If the gain errors vary with array pointing (due to multipath problems), then they will be very difficult to control. These results indicate that gains must be measurable and controllable at a level of a few percent. Potentially, there are algorithms that are robust with respect to gain variations, but we have not identified them.

Measuring the correlation matrix has the advantage of measuring the relative antenna gains at the locations of the interferers (as well as the locations of the interferers). However, this ties up considerable resources. Furthermore, weak interferers are not easily detected and removed from a measured correlation matrix. Determining the correlation matrix from the assumed source position is straightforward and simple computationally. Weak interferers may be treated as strong interferers and solutions are accurately determined. Potentially, a hybrid approach could be employed in which weak interferers of known position are added to a measured correlation matrix.

A small array of omni-directional antennas could add substantially to the capacity to estimate interferer positions. These antennas could perform angle-of-arrival experiments that update interferer location tables. This would be particularly valuable for aircraft whose locations cannot be known *a priori.* The AOA tests must determine locations to an accuracy $\sim 10''$ at 1.4 GHz. The positional accuracy of an AOA experiment will be on the order $\frac{\lambda}{B}\frac{1}{\mathrm{SNR}}$. DME signals detected with the RFI monitor at Hat Creek have SNR ~ 30 dB in 0.1 msec observations. A software correlator could easily update positions every second with $10''$ if $\frac{B}{\lambda} = 10 - 100$. The RPA could serve as a useful testbed for such schemes.

Certain implementations of the digital architecture favor a phase-only gain that can be controlled on short timescales. We will investigate phase-only methods in a future memo.

Finally, we note that implementation of the MV algorithm with an FX correlator could allow for broad band interference mitigation. Gain coefficients could be applied to individual narrow channels either at the correlator input (following the Fourier transform) or at the correlator output (following the multiplication).

4. References

Ellingson, S.W. & Hampson, G.A., 2001, IEEE Ant. Prop., submitted

Godara, L.C., 1997, Proc. IEEE, 85, 1195-1245

Fig. 1.— Antenna positions for ATA k12_1 configuration.

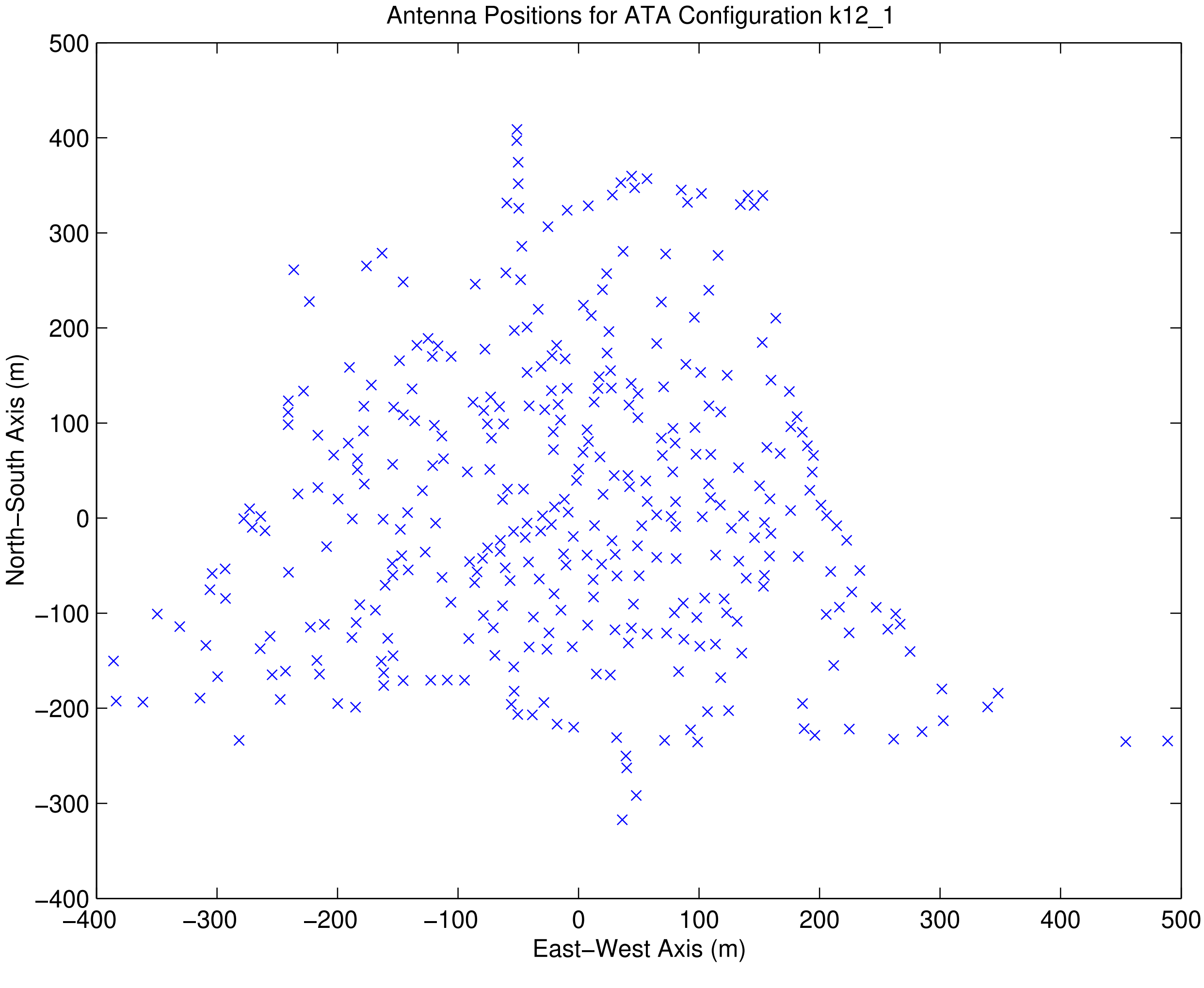

Fig. 2.— Frequency width of a null.

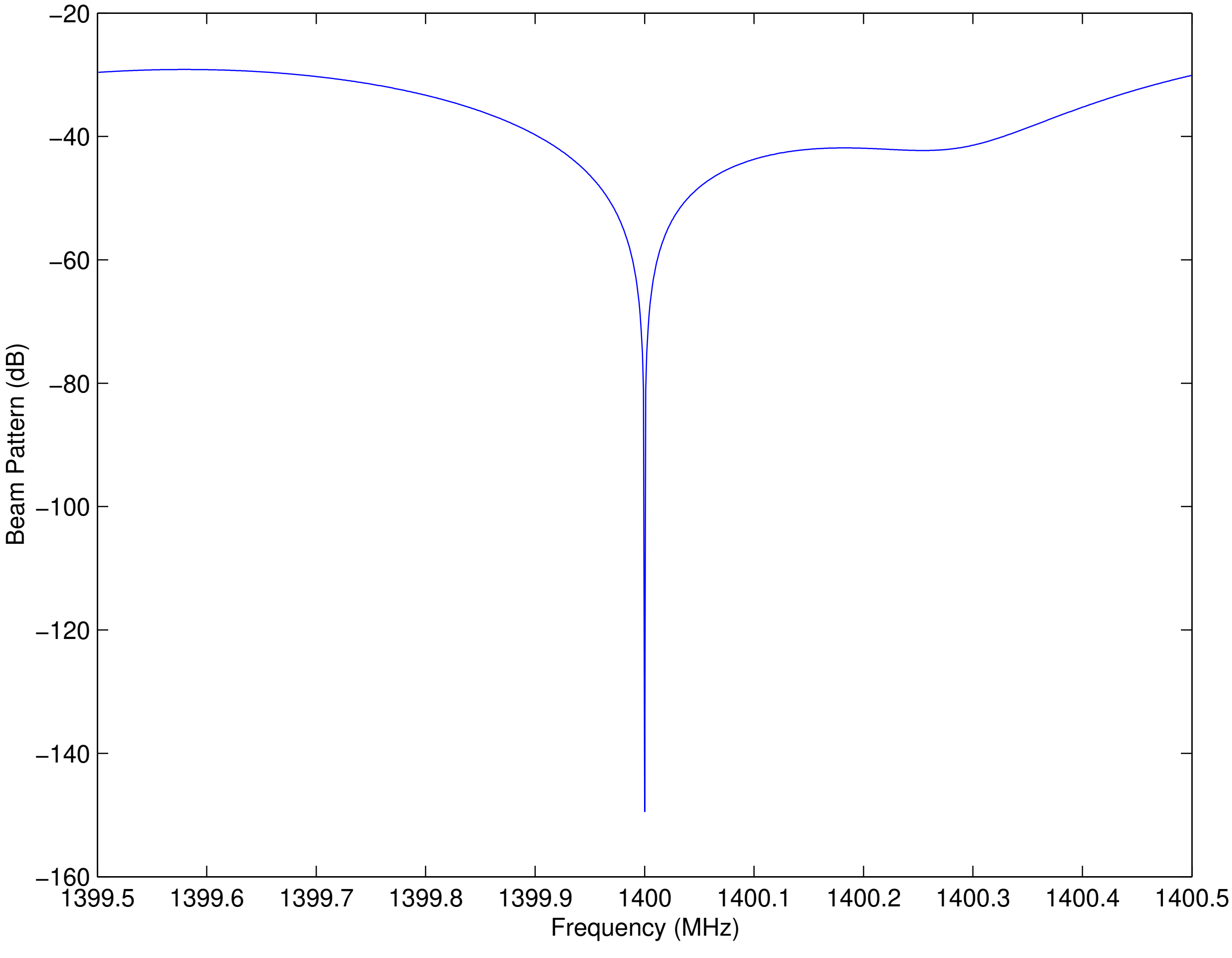

Fig. 3.— Angular width of a null. Z-axis is logarithm of beam pattern response.

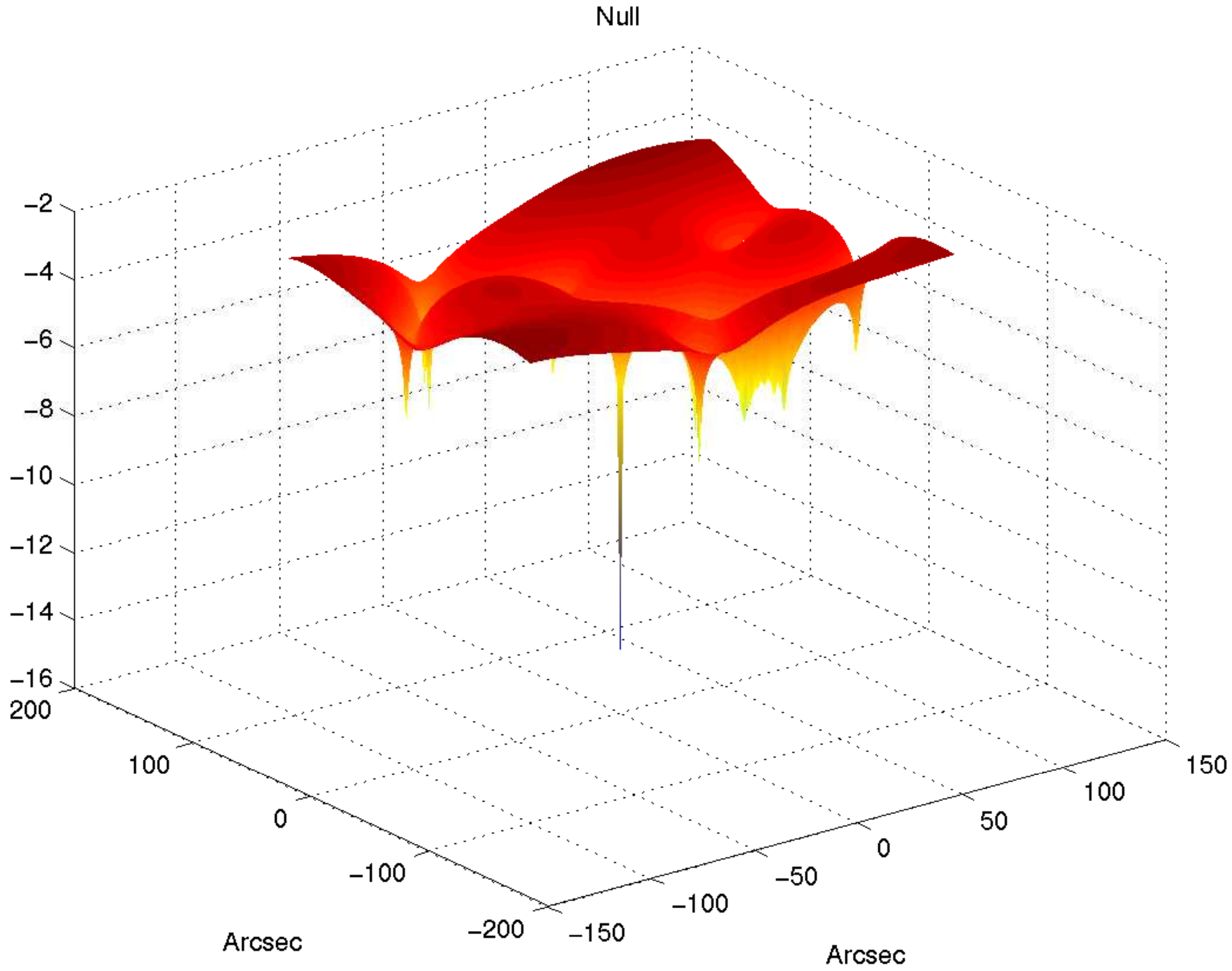

Fig. 4.— Contour image showing angular width of a null placed at the origin. Contours are decibels of beam pattern response.

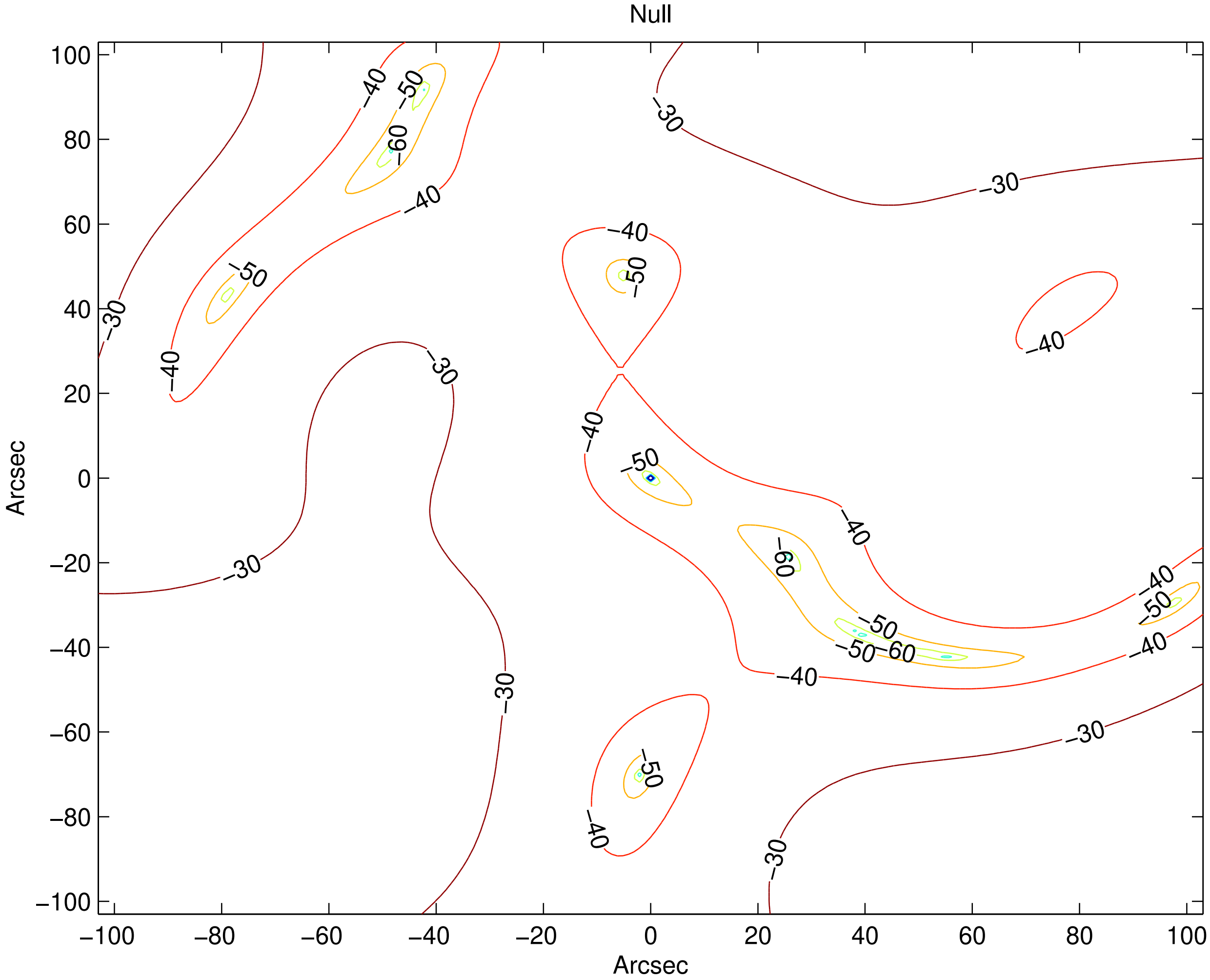

Fig. 5.— Image showing one quarter of the sky with a peak and a single null. X- and Y- axes are direction cosines. Z-axis is logarithm of beam pattern response.

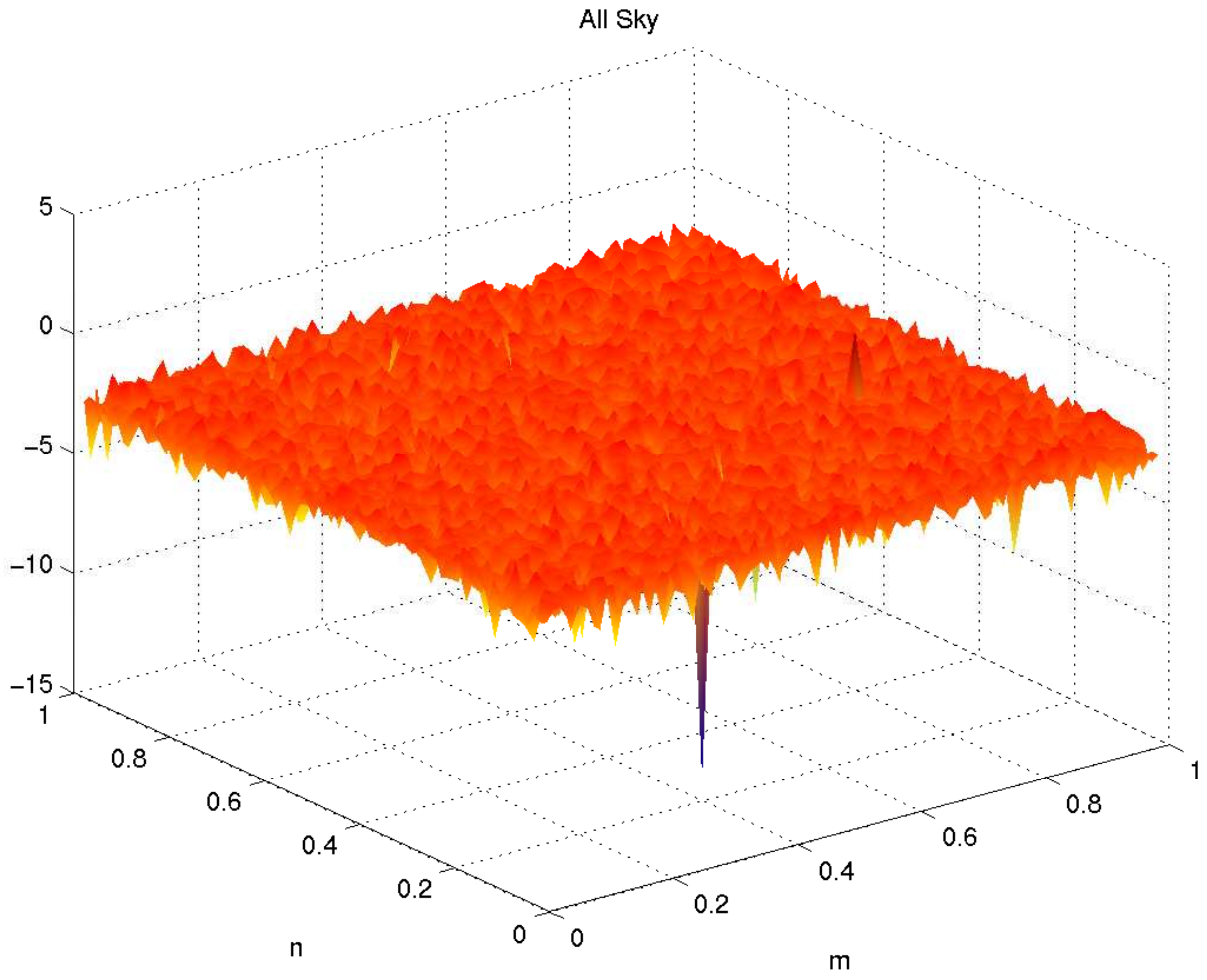

Fig. 6.— Contour image showing angular width of a null formed from five individual nulls. Contours are decibels of beam pattern response.

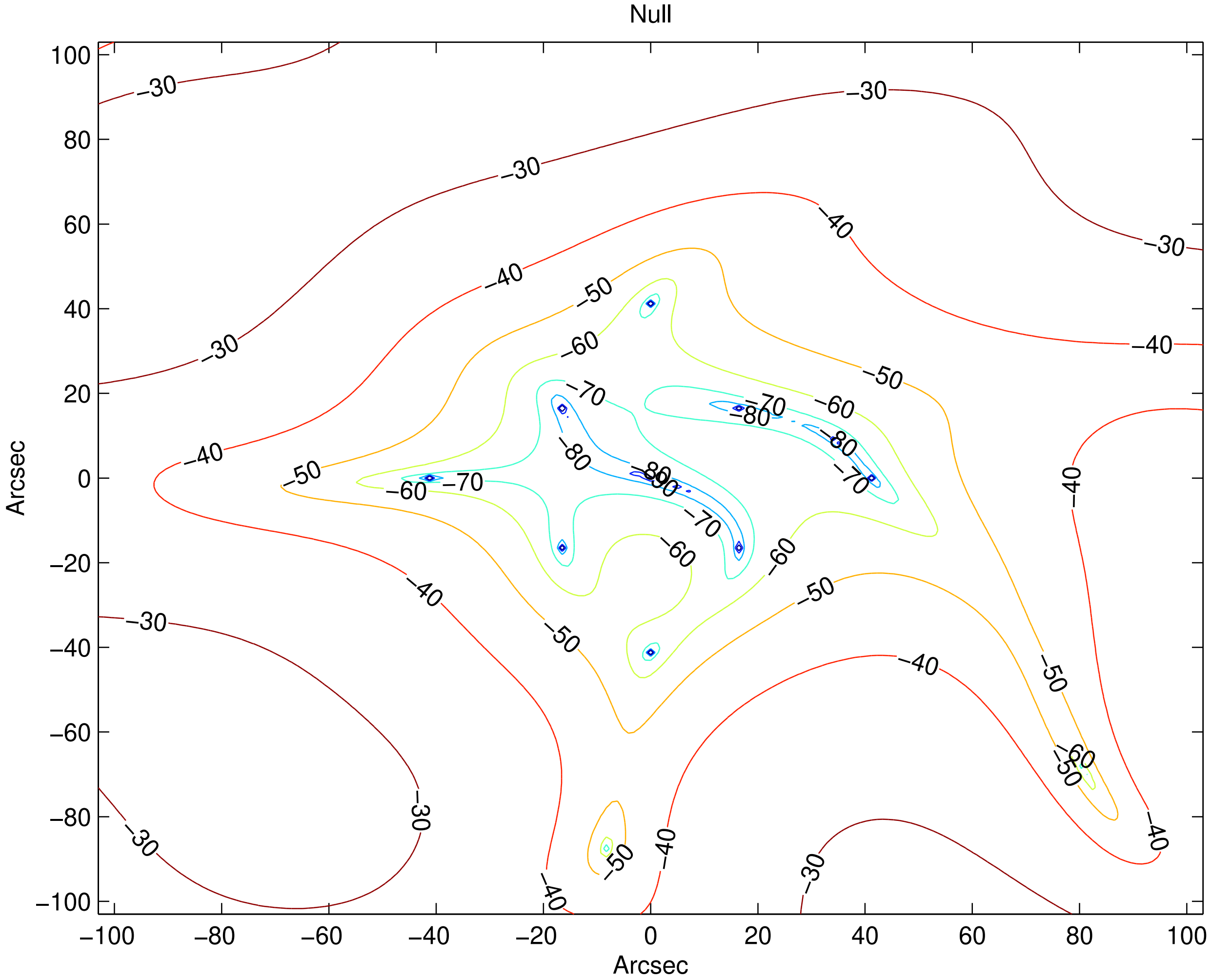

Fig. 7.— Image showing one quarter of the sky with a peak and 15 nulls. Some of the nulls are hidden by the viewing angle. X- and Y- axes are direction cosines. Z-axis is logarithm of beam pattern response.

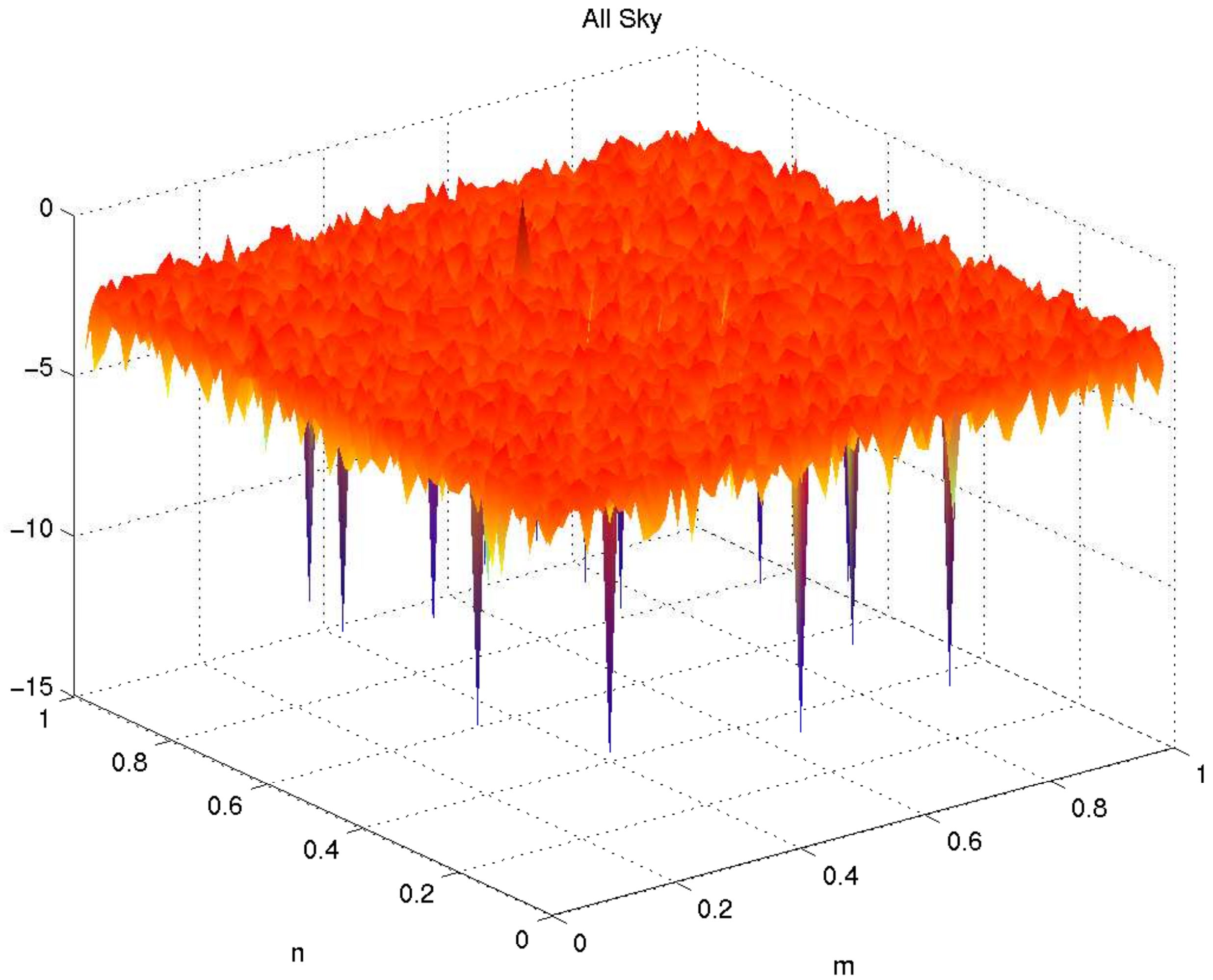

Fig. 8.— Deviation of beam pattern at peak with the addition of one null.

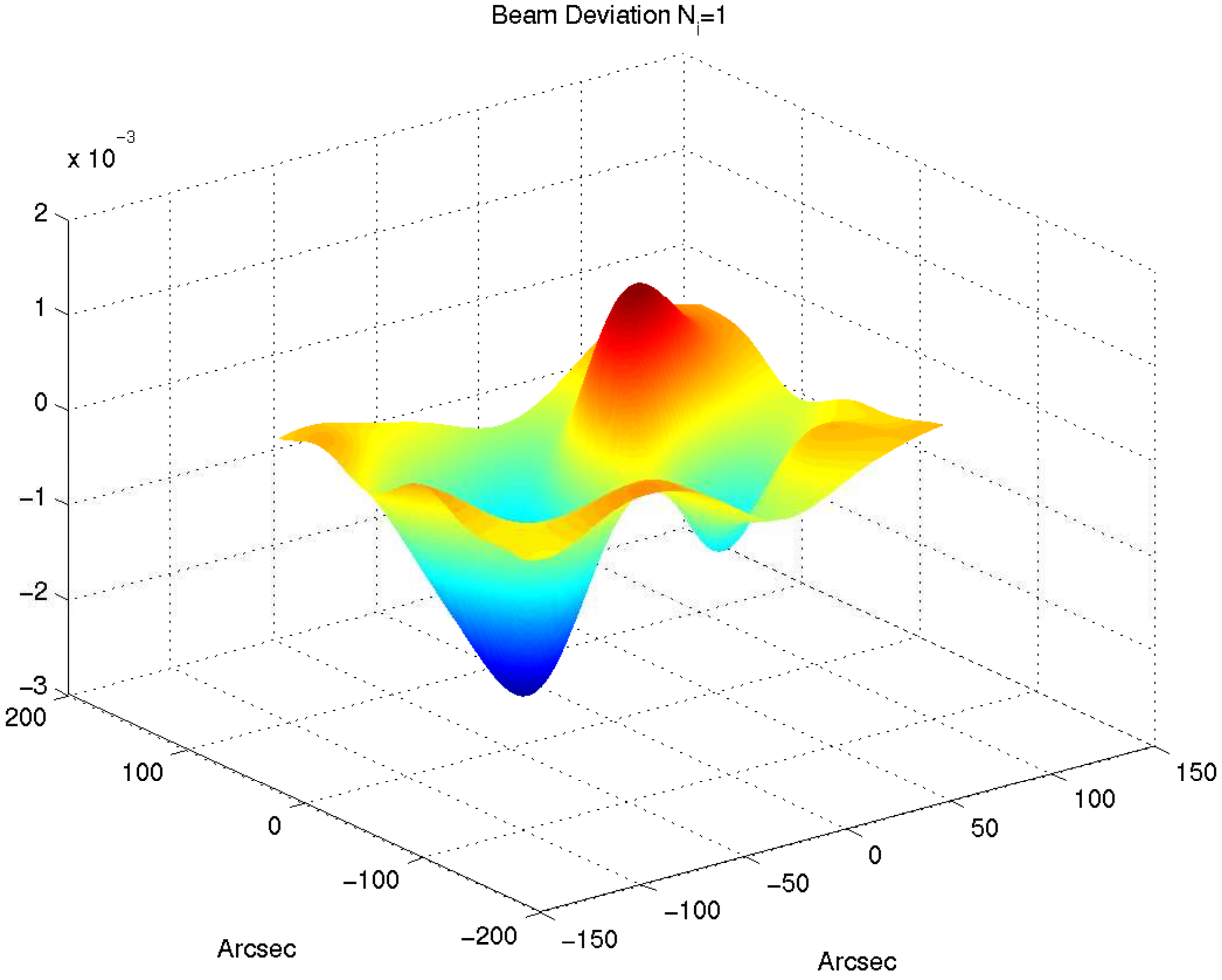

Fig. 9.— Deviation of beam pattern at peak with the addition of 15 nulls.

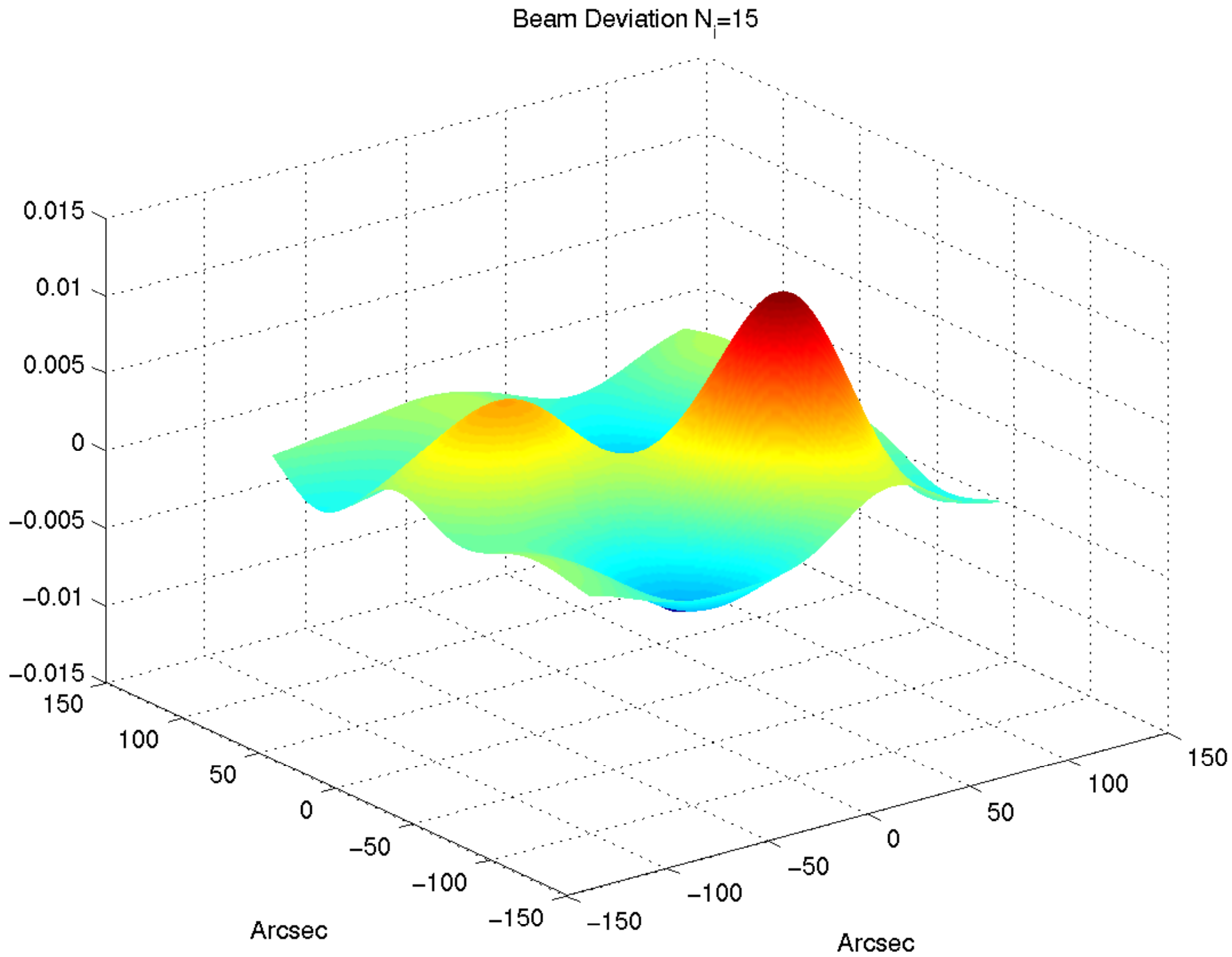

Fig. 10.— Complex patterns can be written with nulls.

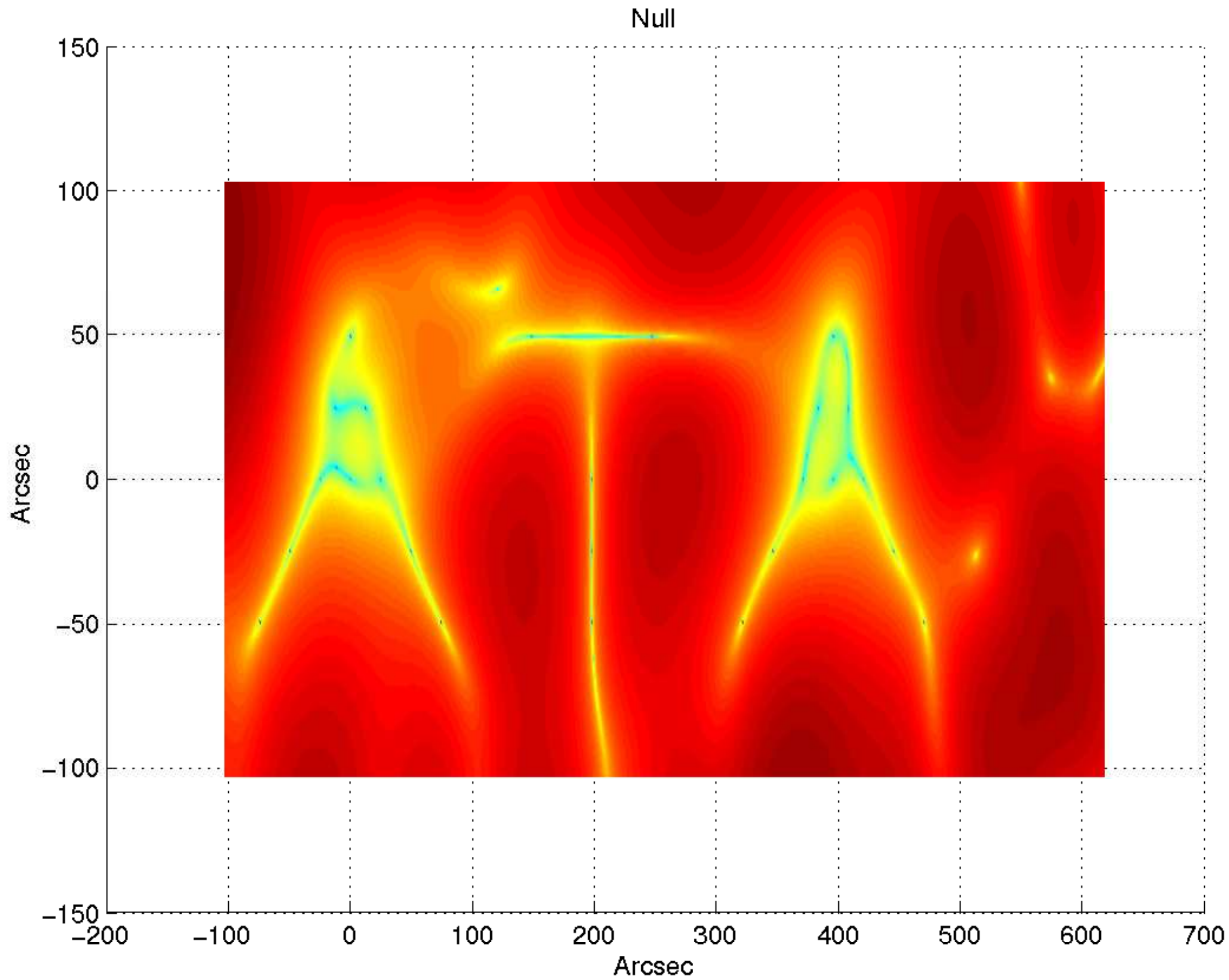

Fig. 11.— The trace of nulls for which the complex gains are interpolated between two endpoints. The interferer moves linearly between the two endpoints but the null does not. Axes are direction cosines.

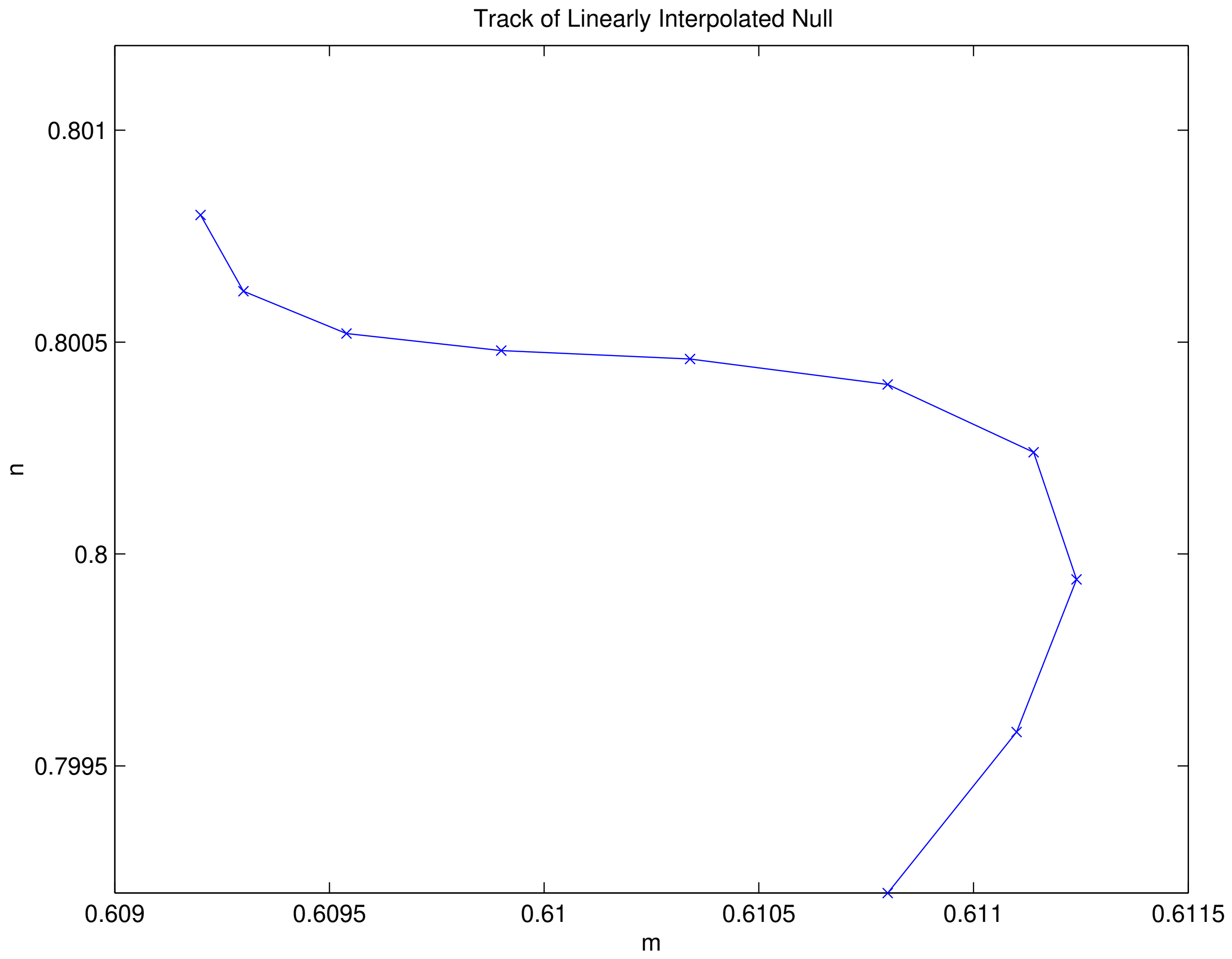

Fig. 12.— Evolution of null parameters for a fixed beam direction and a null tracking a GPS satellite. The upper two panels show the amplitude and phase solutions for five antennas. The middle panels show the structure functions for the amplitude and phase solutions for all antennas. The bottom left panel shows the azimuth and elevation track of the GPS satellite. The bottom right panel shows the SNR on source as a function of time.

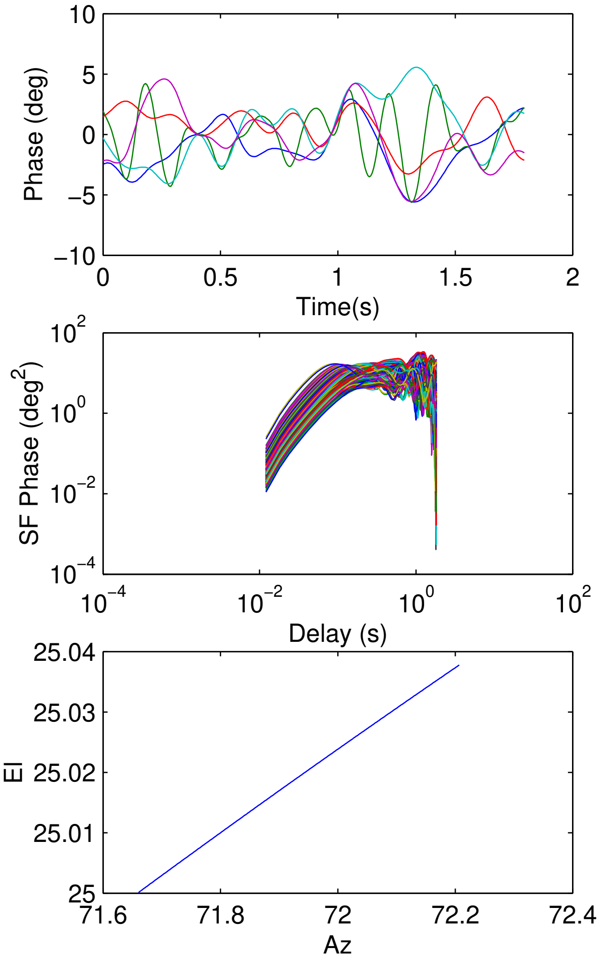

Fig. 13.— Null formed for the path of a GPS satellite. Fifty individual nulls were placed along the 1.5 second path of the GPS satellite.

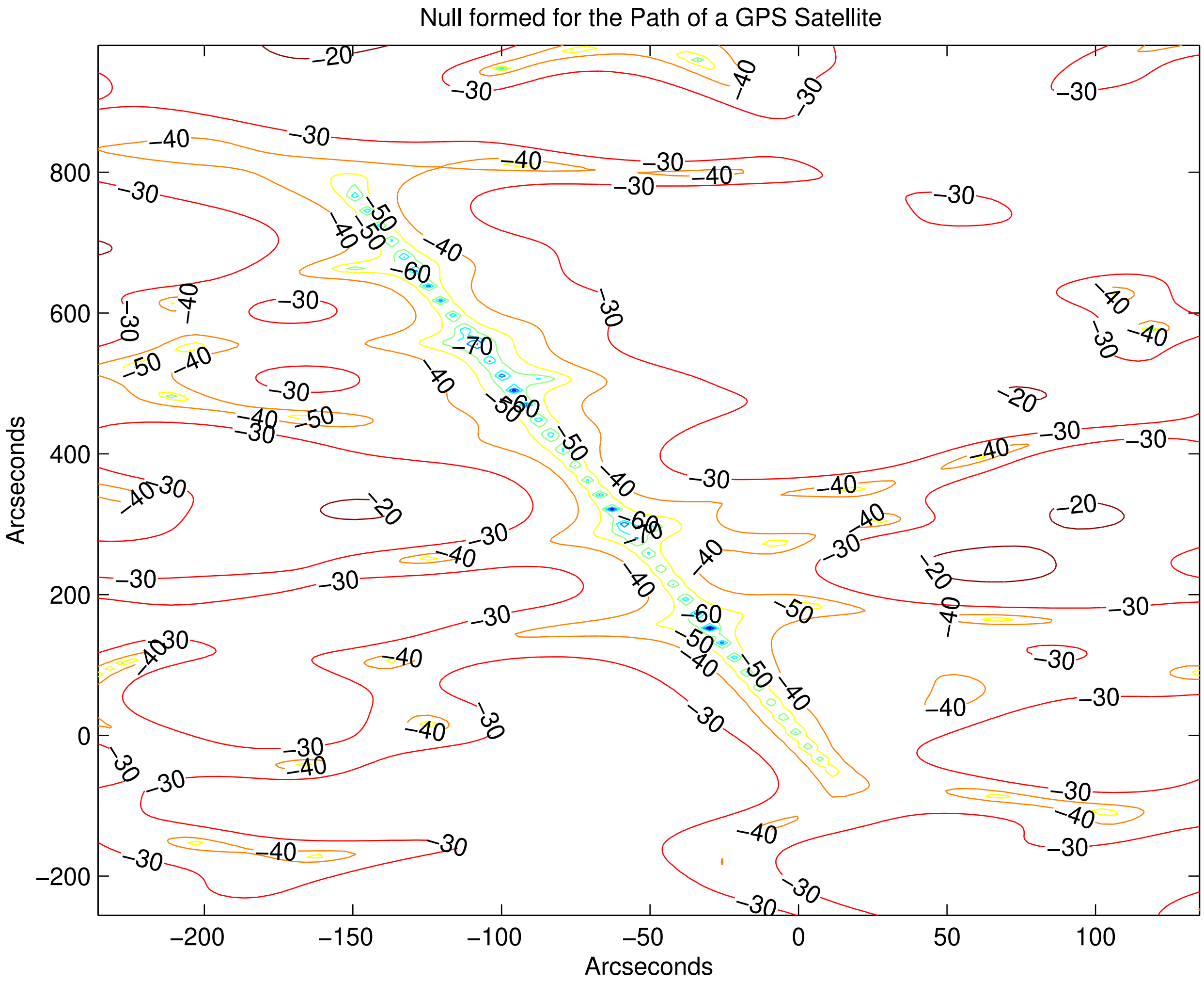

Fig. 14.— SNR at the phase center as a function of number of nulls and number of antennas.